Heliyon 10 (2024) e33381

Contents lists available at ScienceDirect

Heliyon

journal homepage: www.cell.com/heliyon

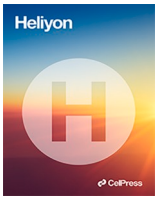

Research article

Enhancing bioactivity and biocompatibility of polyetheretherketone (PEEK) for dental and maxillofacial implants: A novel sequential soaking process

Wenqing Meng, Yifei Nie, Jiajia Zhang, Ludan Qin, Xueye Liu, Tongtong Ma, Junling Wu *

Department of Prosthodontics, School and Hospital of Stomatology, Cheeloo College of Medicine, Shandong University & Shandong Key Laboratory of Oral Tissue Regeneration & Shandong Engineering Research Center of Dental Materials and Oral Tissue Regeneration & Shandong Provincial Clinical Research Center for Oral Diseases, No.44-1 Wenhua Road West, 250012, Jinan, Shandong, China

ARTICLE INFO

Keywords:
Polyetheretherketone (PEEK)
Surface modification
Osseointegration
Antibacterial property

ABSTRACT

Polyetheretherketone (PEEK) exhibits excellent biocompatibility, fatigue resistance, and an elastic modulus similar to bone, presenting broad application prospects in the field of dental and maxillofacial implants. However, the bioinertness of PEEK limits its applications. In this study, we developed a method to generate biocompatible and bioactive PEEK through a simple sequential soaking process, aimed at inducing bone differentiation and enhancing antibacterial properties. Initially, a three-dimensional (3D) porous network was introduced on the PEEK surface by soaking in concentrated sulfuric acid and water. Subsequently, the sulfonated PEEK surface was treated with oxygen plasma, followed by immersion in a dopamine solution to coat a polydopamine (PDA) layer. Finally, polydopamine phosphate ester-modified 3D porous PEEK was obtained through the reaction of phosphoryl chloride with surface phenolic hydroxyl groups. Systematic studies were conducted using scanning electron microscopy, X-ray photoelectron spectroscopy, water contact angle analysis, cell proliferation and adhesion, osteogenic gene expression detection, alkaline phosphatase staining, alizarin red staining, and bacterial culture. Overall, compared to unmodified PEEK, the modified PEEK significantly enhanced in vitro cell proliferation and adhesion, osteogenic differentiation, and antibacterial properties. The simple surface modification measures combined in this study may represent a promising technology and could facilitate the application of PEEK in dental and maxillofacial implants.

1. Introduction

In contemporary dental and maxillofacial implants practice, the widespread utilization of traditional metallic implants like cobalt-chromium-molybdenum and titanium alloys is attributed to their outstanding mechanical attributes and biocompatibility [1,2]. Nonetheless, these alloys can trigger inflammatory responses from the release of metal ions, and their high rigidity may cause stress-shielding effects that lead to bone loss and eventually result in implant failure [3–5]. In order to address these constraints, recent studies have centered on exploring alternative materials as substitutes for metal alloys. In the 1990s, researchers worldwide started

* Corresponding author. No.44-1 Wenhua Road West, 250012, Jinan, Shandong, China.
E-mail address: doctorwujunling@163.com (J. Wu).

https://doi.org/10.1016/j.heliyon.2024.e33381
Received 6 June 2024; Accepted 20 June 2024
Available online 23 June 2024

exploring the potential of polyetheretherketone (PEEK) as a viable dental and maxillofacial implant material [5,6]. PEEK, a thermoplastic substrate with partial crystallinity, demonstrates excellent biocompatibility, fatigue resistance, and an elastic modulus comparable to natural bone [5,7,8]. The elastic modulus of PEEK, at 3–4 GPa, closely matches that of cortical bone (18 GPa), making it a superior choice compared to the much higher moduli of titanium alloy (110 GPa) and cobalt-chromium alloy (200 GPa) [7,9]. This property facilitates the prevention of stress-shielding effects in orthopedic applications [7,9]. Nevertheless, the untreated surface of PEEK exhibits a high level of hydrophobicity, leading to pronounced bioinertness and inadequate bone conduction, thereby restricting its clinical utility [10,11]. To enhance PEEK's bioactivity, surface modification and composite preparation serve as primary strategies [6]. In surface modification, ensuring the stability of the altered surface is a critical aspect that necessitates further exploration. In the development of bioactive PEEK composites, the primary challenge lies in preserving PEEK's outstanding mechanical properties while integrating bioactive materials [6]. For instance, incorporating β-tricalcium phosphate or hydroxyapatite (HA) into PEEK composites can enhance their bioactivity [12,13]. Nevertheless, this method compromises PEEK's tensile strength during the injection molding shapeforming [14,15].

Sulfonation modification entails the brief reaction of PEEK with concentrated sulfuric acid or gaseous sulfur trioxide [16]. This process introduces $–SO_3H$ groups, forming porous structures on PEEK's surface [17,18]. Plasmas, ionized gases generated by stimulating a low-pressure gas mixture with electromagnetic waves in a closed reactor system, can interact with the surface of biomaterials inside the reactor [19]. Plasma treatment enhances PEEK's bioactivity by increasing the hydrophilicity of surfaces, enabling selective cell adhesion, while preserving the material's relevant mechanical, electrical, and optical properties crucial to its application [20–23]. Dopamine is employed to create a functional coating on the surface of PEEK. Dopamine self-polymerizes in alkaline media and subsequently creates a versatile polydopamine (PDA) coating, abundant in catechols, amines, and quinones. Catechol can generate reactive oxygen species to disrupt bacterial cell walls, and PDA can disrupt bacterial structures through ion/protein complexation and electrostatic effects, thereby exerting antibacterial effects [24–26]. Moreover, phosphoryl chloride has been reported as a phosphorylating reagent employed in modifying PEEK surfaces [27,28]. In this specific application, phosphoryl chloride can react with surface hydroxyl groups, introducing phosphate moieties onto the material's surface [27,28]. Cells can detect increased extracellular phosphate concentrations through phosphate transporters, initiating signal transduction pathways associated with osteogenesis and thereby promoting osteogenic differentiation [29,30].

Considering these aspects, this study aimed to synergistically enhance the biocompatibility and antibacterial properties of PEEK by integrating various surface modification techniques mentioned previously, utilizing a sequential soaking process. First, a three-dimensional (3D) porous structure was introduced on the surface of PEEK through sulfonation, then followed by plasma activation of the sulfonated PEEK surface to enable subsequent PDA coating. Lastly, polydopamine phosphate ester was covalently bonded to the PEEK surface through subsequent reactions. A systematic investigation of the modified PEEK involved the characterization of its surface structure, assessing in vitro cellular responses, and evaluating its antibacterial properties.

2. Materials and methods

2.1. Materials

The medical-grade PEEK substrates (Φ 10 mm × 1 mm) were obtained from Shenzhen Wanxin Plastics Co., Ltd. (Shenzhen, China). Acetone, anhydrous ethanol, dichloromethane, and triethylamine in the study were purchased from Shanghai HuShi Laboratory Equipment Co., Ltd. (Shanghai, China). Phosphoryl chloride and concentrated sulfuric acid were provided by Chengdu Kelong Chemical Co., Ltd. (Chengdu, China). Tris-HCl buffered solution and dopamine hydrochloride were supplied by Shanghai yuanye Bio-Technology Co., Ltd. (Shanghai, China). All chemical reagents were used without additional purification, exactly as received. 1 × Phosphate Buffered Saline (PBS, Biosharp, China), α-minimum essential medium (α-MEM, HyClone, USA), Dulbecco's modified Eagle's high glucose medium (DMEM, HyClone, USA), brain heart infusion broth (BHI, Hope bio-technology, China), fetal bovine serum (FBS, Gibco, USA), 4 % Formaldehyde Universal Tissue Fixative (Biosharp, China), penicillin/streptomycin (EveryGreen, China), Cell Counting Kit-8 (CCK-8, Biosharp, China), 4',6-Diamidino-2-Phenylindole (DAPI, Beyotime, China), Calcein AM/PI Double Staining Kit (Elabscience, China), BCIP/NBT Alkaline Phosphatase Color Development Kit (BCIP/NBT Kit, Beyotime, China), Ascorbic acid (Vitamin C, Solarbio, China), β-Glycerol phosphate disodium salt pentahydrate (β-GP, Solarbio, China), dexamethasone (Sigma-Aldrich, USA), 2 % Alizarin Red S Staining Solution (LEAGENE, China), Trizol (Thermo Fisher, USA), Hifair® III 1st Strand cDNA Synthesis SuperMix for qPCR (gDNA digester plus) (YEASEN, China), and Hieff Unicon® Universal Blue qPCR SYBR Green master mix (YEASEN, China) were also used as received. Primers for quantitative real-time reverse transcription polymerase chain reaction (qRT-PCR) were procured from Boshang Biotechnology Co., Ltd. (Guangzhou, China).

Staphylococcus aureus (S. aureus), escherichia coli (E. coli), mouse fibroblast L929 cells, and mouse preosteoblasts MC3T3-E1 cells were provided by Shandong Engineering Research Center of Dental Materials and Oral Tissue Regeneration. Approval for the use of these materials was granted by the Medical Ethics Committee of Shandong University School of Stomatology.

2.2. Preparation of modified PEEK

PEEK substrates underwent polishing using SiC paper (#800) and were subsequently subjected to sequential ultrasonic cleaning sessions (SB4200D, SCIENTZ, China) lasting 30 min each in acetone, anhydrous ethanol, and deionized water. The cleaned PEEK substrates were dried in an electric thermostatic drying oven (DFA-7000, RUIDIAN, China) at 37 °C for later use. At room temperature, the specimens were immersed in concentrated sulfuric acid within an ultrasonic bath for a duration of 3 min. Afterward, they

underwent sequential ultrasonic cleaning in deionized water, anhydrous ethanol, and deionized water, each for 10 min, and subsequently they were dried for 1 h (denoted as SPEEK). Plasma treatment was conducted employing a plasma surface treatment processor (Atto, Diener, Germany) at 50 kHz and electric power of 100 W under an airflow at 20 sccm at 0.01 T for 2 min to produce hydroxyl groups (labeled as pSPEEK). Then, 400 mg of dopamine hydrochloride was dissolved in 200 mL of 10 mM Tris-HCl buffered solution (pH 8.5) to prepare a 2 g/L dopamine solution. Specimens were immersed in the solution and shaken (80 rpm) for 24 h with avoidance of light exposure under ambient conditions. On the following day, the specimens underwent three 15-min sonication cycles in deionized water and were subsequently dried in a vacuum drying oven (ZKXF, SHULI, China) for 1 h (designated as pSPEEK-PDA). The specimens with prepared PDA coatings were immersed in 100 mL of dichloromethane containing 1.535 g of phosphoryl chloride and 1.01 g of triethylamine, and then stirred at 80 rpm for 24 h at room temperature while protecting from light exposure [28]. Following the cleaning of the treated substrates using acetone and deionized water, they were subjected to vacuum drying, leading to the formation of PEEK with polydopamine phosphate ester coatings (termed as pSPEEK-PPE). The designations and respective processing procedures for each specimen group were presented in Table 1.

2.3. Surface characterization

Following a 60-s metal sputtering process, the surface topography of the prepared specimens was investigated utilizing a scanning electron microscope (SEM) (JSM-7610F, JEOL Ltd., Japan) at the accelerating voltage of 5 kV. The surface chemical compositions were analyzed through X-ray photoelectron spectroscopy (XPS) (K-Alpha, Thermo Fisher Scientific, USA). Charge correction was conducted using C1s (284.8 eV) as a reference, and fitting analysis was performed using XPS Peak 4.1 software. The surface wettability of the specimens was evaluated by measuring the contact angles of 2 μL water droplets using a contact angle meter (OCA40, Dataphysics, Germany). Contact angle measurements were conducted on randomly selected regions of each specimen.

2.4. Cell study

2.4.1. Cell culture

L929 fibroblasts were cultured in a complete medium (89 % DMEM high glucose medium, 10 % FBS, and 1 % penicillin/streptomycin). The culture was sustained at 37 °C in an atmosphere of 5 % CO_2 and 95 % air [31]. The culture conditions for MC3T3-E1 osteoblasts were identical to those of L929 fibroblasts, except for replacing DMEM high glucose medium with α-MEM. The culture medium was renewed every 48 h until cells reached desired confluence.

2.4.2. Cell proliferation

Prior to tests, specimens were washed with deionized water, PBS, and 75 % ethanol, and then irradiated on both sides under ultraviolet light for 1 h each. The proliferation of L929 and MC3T3-E1 cells on the prepared specimens was quantitatively assessed using the CCK-8 kit. In 24-well tissue culture plates, each specimen was seeded with cell suspensions (1 mL) containing 2×10^4 cells per well. On days 1, 4, and 7, the number of viable cells was quantified using 96-well tissue culture plates according to the manufacturer's instructions. The absorbance at a wavelength of 450 nm was determined using a microplate reader (SPECTRO star Nano, BMG Labtech, Offenburg, Germany) [32,33]. For each group, the final data was derived by deducting the values obtained from the negative control group from the corresponding measured values.

2.4.3. Cell adhesion

In 24-well plates, 2×10^4 L929 and MC3T3-E1 cells were seeded on the surfaces of different groups of specimens and co-cultured in direct contact for 4 h, 24 h, and 72 h. Following this, the cells were rinsed with PBS and then fixed for 30 min using 4 % paraformaldehyde. Afterward, cell nuclei were observed through staining with DAPI. Similarly, after 24 h of culture, live and dead cells were stained with the Calcein AM/PI Double Staining Kit as per the guidelines provided by the manufacturer. A fluorescence microscope (D-35 578, Leica, Wetzlar, Germany) was used to capture images of the cells present on the specimen surfaces.

2.4.4. Quantitative real-time polymerase chain reaction (qPCR) for osteogenic gene expression detection

In 24-well plates, 2×10^4 MC3T3-E1 cells per specimen ($n = 3$) were seeded and cultured for 7 and 14 days. At the indicated time interval, the total ribonucleic acid (RNA) was extracted using Trizol reagent. The complementary deoxyribonucleic acid (cDNA) was reverse-transcribed from the collected RNA using the Hifair® III 1st Strand cDNA Synthesis SuperMix for qPCR (gDNA digester plus),

Table 1
The designations and respective processing procedures for each specimen group.

Designation	Processing Procedure
PEEK	Pure PEEK
SPEEK	PEEK → Sulfonation
pSPEEK	PEEK → Sulfonation → Oxygen plasma treatment
pSPEEK-PDA	PEEK → Sulfonation → Oxygen plasma treatment → PDA coating
pSPEEK-PPE	PEEK → Sulfonation → Oxygen plasma treatment → PDA coating → Phosphorylation

following the prescribed methods. Primers for both forward and reverse were used for the genes listed in Table 2. The gene expression for osteogenesis-associated genes, such as alkaline phosphatase (ALP), osteopontin (OPN), runt-related transcription factor 2 (Runx2), and type I collagen α 1 (Col1α1) was quantified. Gene expression was analyzed with quantitative real-time PCR (qPCR), employing glyceraldehyde-3-phosphate dehydrogenase (GAPDH) as the housekeeping gene and using the Hieff Unicon® Universal Blue qPCR SYBR Green master mix.

2.4.5. Alkaline phosphate (ALP) and alizarin red (AR) staining of MC3T3-E1 cells

2×10^4 MC3T3-E1 cells were seeded onto specimens and placed in 24-well plates. Medium was refreshed twice weekly with osteogenic induction medium. Osteogenic induction medium consisted of α-MEM, supplemented with 10 % FBS, 10 mM β-GP, 10 nM dexamethasone, and 50 mg/L Vitamin C. At 7 and 14 days post-seeding, ALP staining was performed using the BCIP/NBT kit and calcium nodules were stained with alizarin red. Briefly, cells were fixed and immersed in dyeing solution for 30 min following the protocol outlined in the instruction manual. Excess stain was removed by washes with PBS. Finally, the specimens were observed by a microscope (D-35 578, Leica, Wetzlar, Germany).

2.5. Antibacterial properties evaluation

2.5.1. Antibacterial rate determination

S. aureus and E. coli were chosen as the test microorganism for antibacterial evaluations. In brief, the bacteria precultured in a frozen state were inoculated onto nutrient agar plates and incubated at 37 °C for 24 h in a constant temperature incubator (BI–120F, YIHENG, China). One bacterial colony was transferred into a new liquid BHI medium and then incubated for an additional 24 h under identical conditions. After ultraviolet irradiation, the five sets of specimens were individually immersed in centrifuge tubes containing 2 mL of bacterial suspension (1×10^6 CFU/mL). After a 24 h incubation, the specimens underwent triple rinsing with PBS to eliminate surface-floating bacteria. They were then transferred into centrifuge tubes containing 5 mL of PBS buffer and subjected to ultrasonic agitation for 15 min to detach the bacteria adhering to the specimen surfaces. The shaking solution was diluted 100-fold with sterile PBS, followed by plating 50 μL of the resulting diluted solution. Bacterial colony counting was conducted after being cultured for 24 h. The antibacterial rate (Rp) was calculated by using the following equation [32]: $Rp = (E\text{-}F)/E \times 100\ \%$, where F and E denote the mean bacterial colony counts on the nutrient agar plates' surfaces for the experimental and control groups, respectively.

2.5.2. Bacterial morphology observation

Specimens from each group, post ultraviolet irradiation, were placed in 24-well tissue culture plates. In each well, 2 mL of bacterial suspension (prepared following the method outlined in section 2.5.1., with a concentration of 1×10^6 CFU/mL) was added. After a 24 h incubation, the specimens were gently rinsed three times with PBS and fixed with 4 % polyoxymethylene for 2 h. Subsequently, a series of ethanol solutions (30, 50, 70, 80, 90, and 100 % v/v) was used for sequential dehydration. Before observing the bacterial morphology by SEM (JSM-7610F, JEOL Ltd., Japan), the specimens were sputter-coated with gold [9].

2.6. Statistical analysis

All of the experiments were independently conducted in triplicates, and each data point was presented as averages ± standard deviations based on three replicated measurements. Statistical significance was determined using one-way ANOVA analysis in GraphPad Prism 10.1 software. A p value below 0.05 was considered statistically significant.

3. Results

3.1. Surface modification and characterization

Surfaces of unmodified and modified PEEK were examined by SEM, as depicted in Fig. 1. Upon treatment with concentrated sulfuric acid, the specimen's surface morphology evolved from the smooth texture depicted in Fig. 1a–a 3D porous network with pore sizes between 1 and 2 μm, as presented in Fig. 1b. Subsequent oxygen plasma treatment induced only minor changes in the specimen's surface structure, maintaining the pore size, as demonstrated in Fig. 1c. Contrarily, the introduction of PDA led to a significant alteration in the surface morphology of pSPEEK-PDA, distinct from both SPEEK and pSPEEK, as evidenced in Fig. 1d. Furthermore, Fig. 1e reveals that the interaction between phosphoryl chloride and PDA resulted in an even more pronounced change, endowing the

Table 2
Primer pairs used in quantitative reverse transcription-PCR (qRT-PCR).

Gene	Forward (5'–3')	Reverse (5'–3')
ALP	GCACCTGCCTTACCAACTCT	GTGGAGACGCCCATACCATC
Runx2	GGGACTGTGGTTACCGTCAT	ATAACAGCGGAGGCATTTCG
OPN	CACATGAAGAGCGGTGAGTCT	CCCTTTCCGTTGTTGTCCTG
Col1α1	CCCTGGTCCCTCTGGAAATG	GGACCTTTGCCCCCTTCTTT
GAPDH	TGTCTCCTGCGACTTCAACA	GGTGGTCCAGGGTTTCTTACT

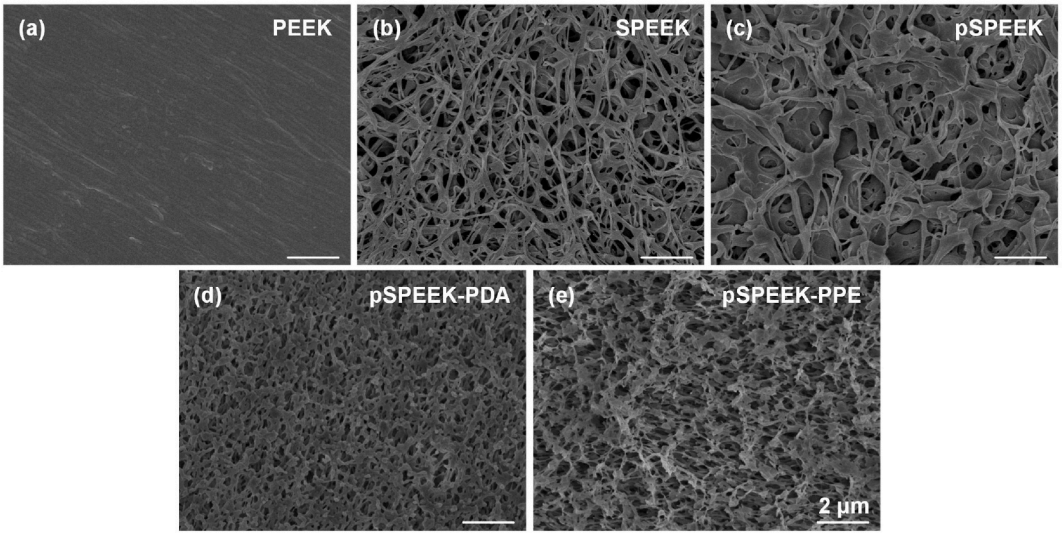

Fig. 1. Scanning electron microscopy (SEM) photographs of the surface of PEEK at different stages of surface modification: (a) PEEK, (b) SPEEK, (c) pSPEEK, (d) pSPEEK-PDA, and (e) pSPEEK-PPE. Scale bars, 2 μm.

pSPEEK-PPE surface with a rougher and more intricate structure.

In Fig. 2, the XPS high-resolution spectra of O 1s, S 2p, N 1s, P 2p for the specimens are displayed, highlighting the impact of different PEEK surface modifications on its chemical composition and elemental configurations at the surface. Specifically, Fig. 2a identifies two distinct peaks at 168.9 and 170.1 eV within the sulfonated SPEEK, aligning with sulfur's $2p_{3/2}$ and $2p_{1/2}$ orbitals. Post oxygen plasma treatment, as depicted in Fig. 2b, the O 1s spectrum showcases a 531.1 eV peak, aligning with hydroxyl groups, alongside a 533.2 eV peak indicating the retention of sulfonic acid groups from earlier stage. Upon applying a PDA coating, the N 1s spectrum in Fig. 2d exhibits a significant peak at 400.1 eV, signifying surface-bound amino groups, thereby partially validating the successful synthesis of pSPEEK-PDA. Notably, a subtle peak at 401 eV hints at the existence of minor by-products like protonated amines or pyridinic nitrogen due to the reaction's complexity. In the context of phosphoryl chloride treatment, as shown in Fig. 2e, the P 2p spectrum of pSPEEK-PPE reveals two salient peaks at 133.7 and 134.6 eV, corresponding to the $2p_{3/2}$ and $2p_{1/2}$ states of phosphorus. Moreover, the O 1s spectrum in Fig. 2c of pSPEEK-PDA illustrates three binding energy peaks at 533.1, 532, and 531.1 eV, associated with O═C, O–H, and O–C. Contrastingly, in Fig. 2f, the O–H characteristic peak in pSPEEK-PPE post phosphoryl chloride treatment exhibits both a reduction in peak area and a positional shift, further corroborating alterations in elemental states and the interaction of hydroxyl groups with phosphoryl chloride.

Fig. 3 illustrates the water contact angles for variously modified specimens, indicating a concerted alteration in surface wettability due to changes in surface morphology and chemical composition. The sulfonation process transitioned the surface wettability from PEEK's hydrophilic state (78.0 ± 1.3°) to SPEEK's hydrophobic nature (112.5 ± 3.0°). Oxygen plasma treatment notably enhanced SPEEK's hydrophilicity, as reflected by the increase in water contact angles, reaching up to 19.8 ± 1.1°. The formation of a PDA coating on the pSPEEK surface further decreased the contact angle to 13.4 ± 1.0°, indicating increased hydrophilicity. Moreover, the integration of phosphate groups into pSPEEK-PPE slightly elevated its contact angle to 25.8 ± 1.7°, yet the material maintained a considerably hydrophilic character.

3.2. Cell study

The proliferation and adhesion of cells are shown in Fig. 4. Fig. 4a depicts the metabolic activity of MC3T3-E1 and L929 cells on various specimens over time, revealing parallel proliferation trends across both cell types at 1, 4, and 7 days, with notably higher metabolic activity in L929 cells. During the initial 1 and 4-day periods, the modified specimens exhibited a degree of cytotoxicity relative to the PEEK control, most pronounced in the SPEEK and pSPEEK groups, as evidenced by a marked decrease in activity. The pSPEEK-PPE group initially displayed cytotoxic effects on day 1, which significantly reduced by day 4. Importantly, at the 7-day mark, the metabolic activities on all modified specimens surpassed those of the PEEK control, indicating that the modifications effectively enhanced cell metabolism and fostered cell proliferation. Fig. 4b and c illustrate DAPI staining on the surfaces of various specimens for MC3T3-E1 and L929 cells at intervals of 4 and 24 h of culture. Fig. 4d, on the other hand, reflects the situation of Calcein AM/PI dual staining at 24 h. The pSPEEK-PPE group, influenced by a combination of surface treatments, exhibited notably enhanced cell adhesion. Initially, at the 4-h mark, the SPEEK and pSPEEK groups did not show significant deviations in cell adhesion compared to the control. However, early-stage cell adhesion was notably facilitated by the modified pSPEEK-PPE. As the culture duration increased, a denser cellular arrangement emerged on all modified specimen surfaces relative to the PEEK control, with the pSPEEK-PPE group maintaining the highest density and most compact cell arrangement. Furthermore, comparatively speaking, the surfaces of the modified materials

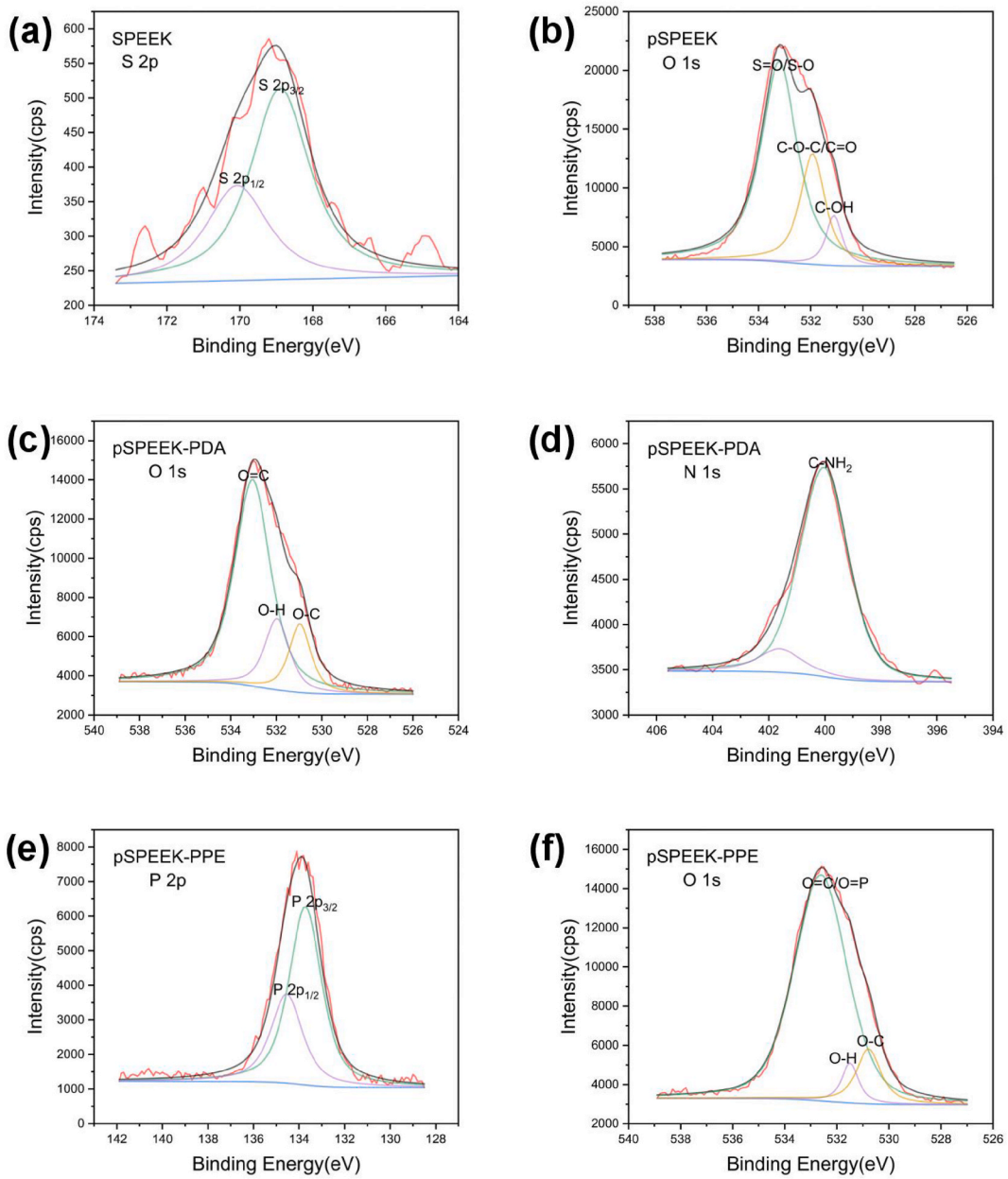

Fig. 2. Chart depicting analytical fitting of XPS test results across various specimen types: (a, b) are for SPEEK and pSPEEK, respectively; (c,d) represent pSPEEK-PDA; and (e, f) stand for pSPEEK-PPE.

more effectively supported L929 cell adhesion, aligning with the CCK-8 kit results shown in Fig. 4a.

Fig. 5 reflects the osteogenic differentiation potential of MC3T3-E1 cells on different specimen surfaces. Osteogenic genes such as ALP, OPN, Runx2, and Col1α1 were assessed on specimen surfaces using RT-PCR (Fig. 5a–d) to determine their expression levels. Following a 7-day exposure to PEEK modified with polydopamine phosphate ester, an increase in the expression levels of ALP and Runx2 was observed in MC3T3-E1 cells. Furthermore, after a 14-day treatment, the levels of OPN and Col1α1 also showed a rise. Contrastingly, MC3T3-E1 cells exposed to unmodified PEEK did not exhibit any changes in the expression of these four osteogenesis-related genes. ALP and AR staining techniques were used to assess the osteoinductive capabilities of PEEK after different modifications. As illustrated in Fig. 5e, on both the 7 and 14 days of cultivation, the specimen surfaces manifested distinct levels of ALP staining intensity. In comparison to the unmodified PEEK control group, the modified PEEK variants displayed a significantly enhanced staining intensity. Notably, these modified specimens demonstrated more conspicuous ALP staining after a 14-day culture period compared to the 7 day, suggesting a time-dependent augmentation in the osteoinductive efficacy of the modified PEEK. Correspondingly, the pSPEEK-PPE showed deeper AR staining (indicative of a deep red coloration) as per Fig. 5f, aligning with the ALP staining trends

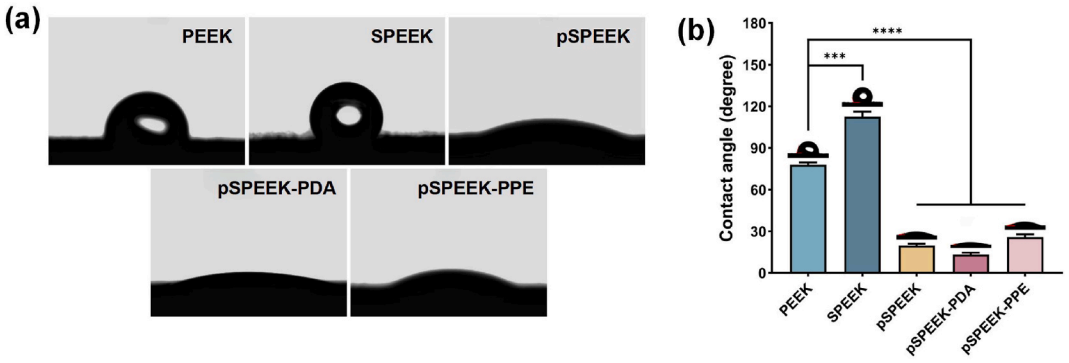

Fig. 3. Water contact angles of different specimens measured by the static sessile drop method: (a) representative pictures of water droplets on different specimens, and (b) statistical analysis, ***P < 0.001, ****P < 0.0001.

depicted in Fig. 5e. Furthermore, these staining results were constant with the RT-PCR results.

3.3. Antibacterial properties evaluation

As shown in Fig. 6, the bacteria cultivation results reflect the antibacterial response of the specimens. Optical imaging of bacterial clones in Fig. 6a reveals a stark contrast: while PEEK harbored numerous S. aureus and E. coli colonies, the counts were markedly lower on SPEEK, pSPEEK, and pSPEEK-PDA, with pSPEEK-PPE exhibiting the minimal bacterial presence. This trend, evident across the specimen groups, shows a consistent reduction in bacterial colony numbers, in alignment with the quantitative data depicted in Fig. 6b and c. Additionally, as calculated and shown in Fig. 6b and c, the antibacterial effectiveness of pSPEEK-PPE against S. aureus and E. coli, compared to the PEEK control, reached an impressive 97.5 ± 1.7 % and 94.4 ± 1.0 %, respectively, further validating its antimicrobial potential. Fig. 6d lucidly presents the SEM observations of S. aureus and E. coli statically cultured on various specimen surfaces. It was observed that the quantity of bacteria adhering to the modified specimens was significantly less than that on the control group. Further, as diverse modification strategies were applied, a steady reduction in bacterial count and a more dispersed arrangement were noted among the groups. In terms of morphology, the bacteria exhibited a clustered and densely packed growth on both the PEEK control and the SPEEK and pSPEEK groups. Contrastingly, the introduction of PDA and PPE modifications led to a noticeable shift in bacterial morphology, making it increasingly irregular and leading to occurrences of shrinkage and rupture.

4. Discussion

Upon implantation of a biomaterial for bone repair into the human body, an immediate interaction is initiated between the material's surface and the surrounding cells [34]. Additionally, aseptic loosening and infection are the primary causes of implant surgery failures [35]. Aseptic loosening typically arises from issues such as prosthetic fretting, inflammatory responses, and bone resorption triggered by wear particles, alongside inadequate bone integration [5,7,35]. Infections near the prosthesis are predominantly initiated by microorganisms, with bacteria adherence to the prosthetic surface being a major contributor. This research aims to enhance this interaction, inhibit bacterial infections, and promote bone integration through straightforward surface modifications. It has been reported that a 3D porous network on PEEK surfaces is typically formed through treatment with concentrated sulfuric acid and subsequent water immersion [36,37]. This modification has been resulted in a sulfonation depth of approximately 30 μm and an open porosity of 1.5 %, indicating a surface-specific treatment that preserves the bulk structure [26]. XPS analysis demonstrates a S 2p spectral peak for HSO_3 groups on the SPEEK surface, marking a change in the chemical composition. Additionally, alterations in the surface morphology and chemistry significantly impact SPEEK's surface wettability. The hydrophilic HSO_3 groups on the SPEEK surface, despite increasing the water contact angle, highlight the pivotal role of the 3D porous network in affecting hydrophilicity. The introduction of surface roughness, although beneficial, was initially counteracted by the residual acids, negatively impacting cell proliferation. To activate the sulfonated surface of SPEEK, oxygen plasma treatment was applied, augmenting SPEEK's hydrophilicity through the addition of hydroxyl groups and thereby enhancing pSPEEK's wettability [22,38]. A subsequent step involved the application of a PDA coating enriched with phenolic hydroxyl groups on the activated surface, creating additional reactive sites [34]. These modifications led to observable changes in pSPEEK-PDA's surface morphology, chemical composition, and wettability, corroborated by SEM, XPS, and water contact angle data. Similarly, the synthesis of phosphorylated PEEK has been realized through the chemical interaction of introduced hydroxyl groups with phosphoryl chloride, a process which notably improves its biological activity [28]. In the present study, the chemical binding of phosphoryl chloride to the reactive sites (phenolic hydroxyl group) on the pSPEEK-PDA surface resulted in the formation of a biomolecular layer, as evidenced by alterations in the O 1s spectrum and the emergence of a P 2p peak around 133–135 eV, confirming the successful integration of phosphate ester groups onto the modified material's surface.

Enhanced cell adhesion and proliferation are associated with factors such as the chemical composition of the surface, its wettability, and roughness. Research shows that cells adhere and proliferate more effectively on hydrophilic surfaces than on hydrophobic

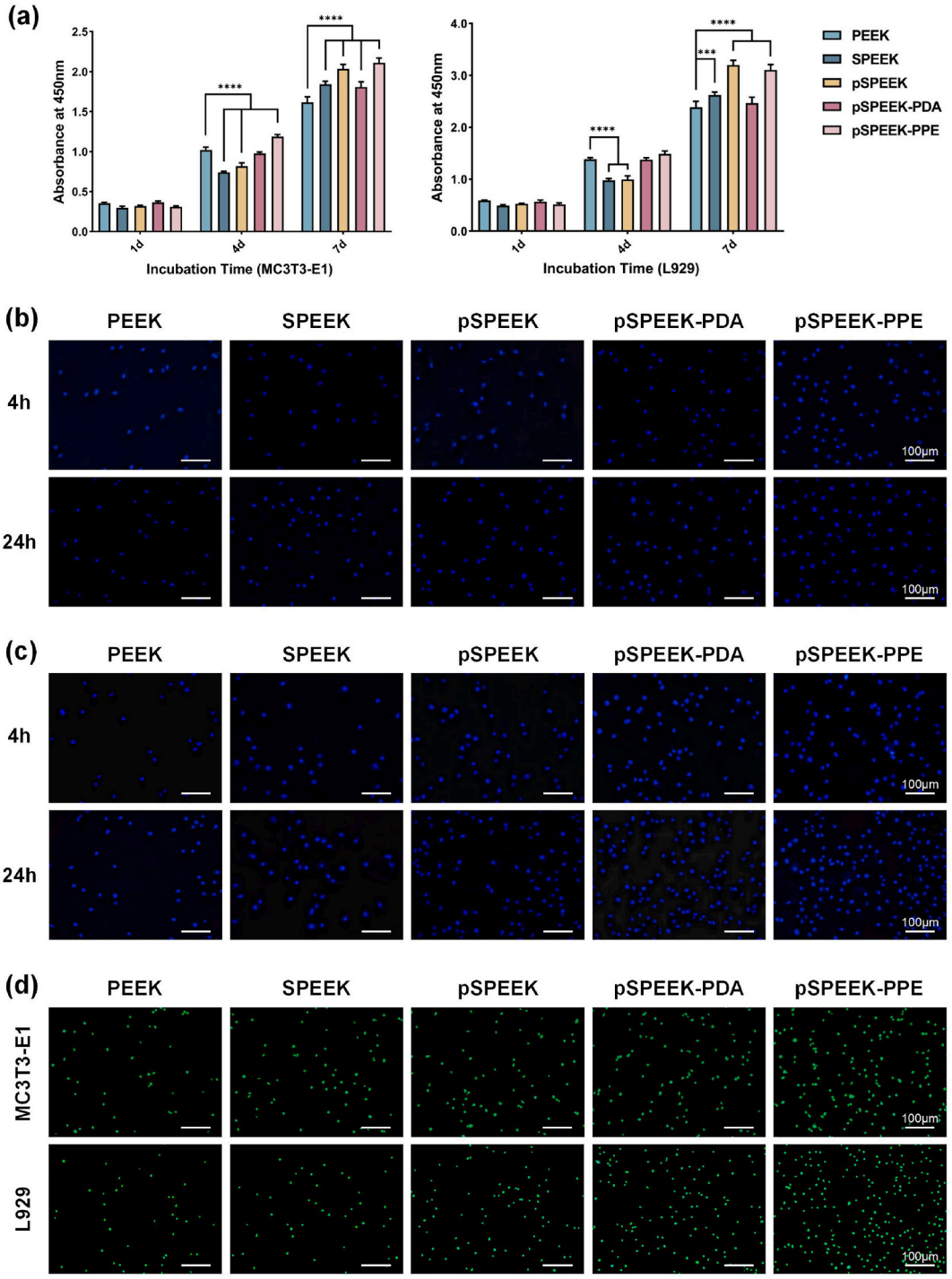

Fig. 4. The proliferation and adhesion status of cells: (a) proliferation of MC3T3-E1 osteoblasts and L929 fibroblasts on the PEEK at different surface modification stages over time intervals (1, 4, and 7 days) measured by the CCK-8 kit at 450 nm absorbance; (b) images of DAPI staining of MC3T3-E1 osteoblasts and (c) L929 fibroblasts cultured on various specimen surfaces for 4h and 24h; and (d) images of Calcein AM/PI dual staining of cells cultured on the surface of PEEK for 24h. ***P < 0.001, ****P < 0.0001. Scale bars, 100 μm.

ones [23]. The wettability of a surface is influenced by its chemical properties and topographical features, including roughness and micro-texture [29]. Hence, it is hypothesized that the beneficial characteristics of the pSPEEK-PPE surface, which support cell adhesion and proliferation, primarily stem from its 3D porous structure and the presence of grafted phosphate groups. Previous research indicates that the chemical composition of a surface plays a crucial role in cell spreading, which significantly influences subsequent

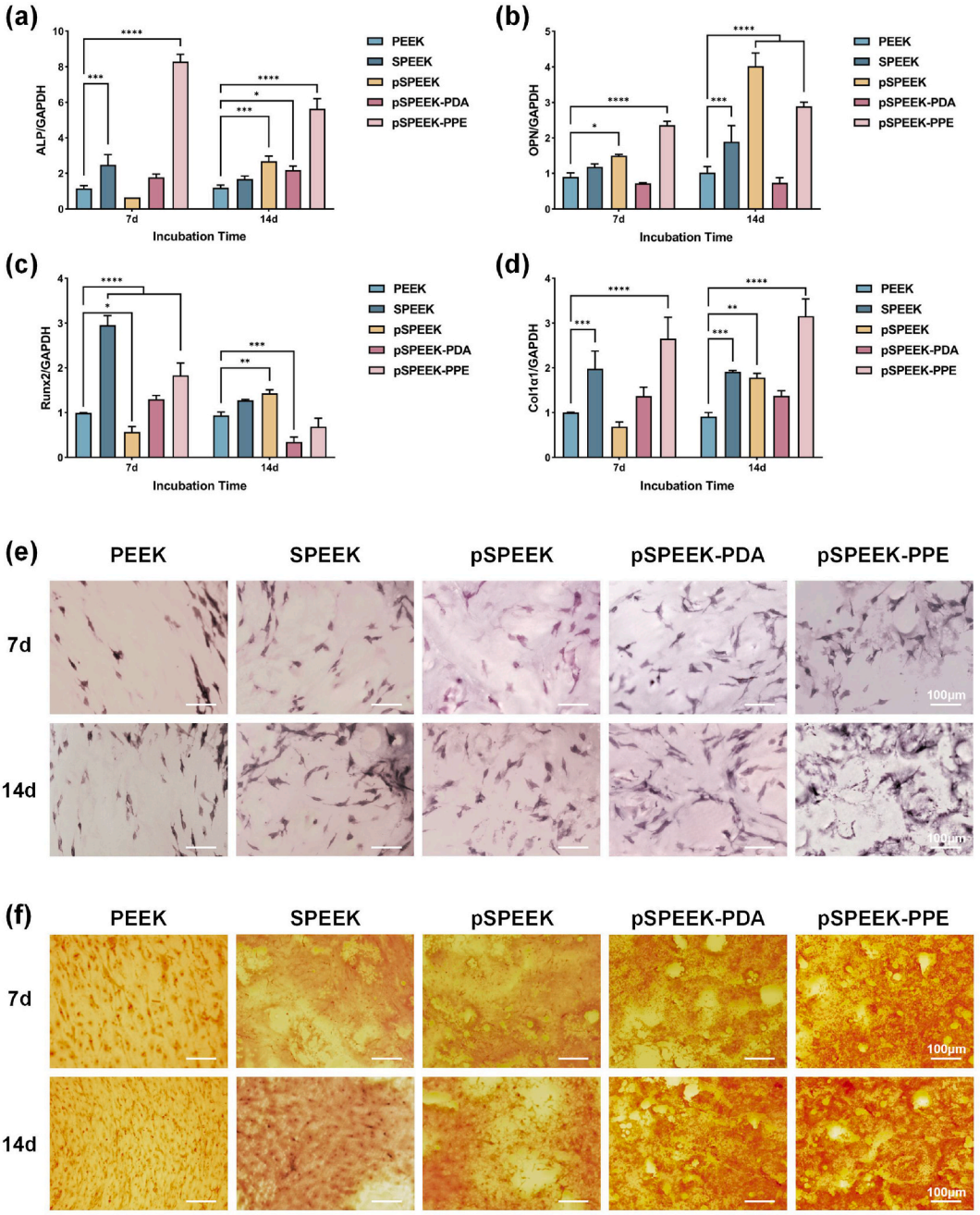

Fig. 5. Osteogenic differentiation assays: (a–d) qPCR detection of osteogenesis-related gene (ALP, OPN, Runx2, and Col1α1 expressions by MC3T3-E1 cells on various surfaces); (e) images of ALP staining observed at 7 and 14 days; and (f) AR staining conducted at 7 and 14 days. *P < 0.05, **P < 0.01, ***P < 0.001, ****P < 0.0001. Scale bars, 100 μm.

processes such as cell adhesion, proliferation, and differentiation [39]. The CCK-8 kit evaluation revealed that the modified specimens initially exerted a detrimental effect on cell proliferation at the early stages, in contrast to the control group. This adverse impact is likely due to the residual sulfur and sulfuric acid not fully eliminated after the sulfonation process. Interestingly, after a period of 7 days, modified specimens, especially those of SPEEK, pSPEEK, and pSPEEK-PPE categories, were found to significantly promote cell proliferation. This beneficial effect can be ascribed to the progressive removal of deleterious substances as the culture medium is refreshed over time, coupled with the beneficial effects of oxygen plasma treatment and the incorporation of phosphate groups, both of which contributed to the enhancement of cell proliferation and adhesion. Additionally, in the Calcein AM/PI dual staining results, it can be observed that there are almost no dead cells on the surface of pSPEEK-PPE, which fully demonstrates its favorable properties for cell adhesion and proliferation.

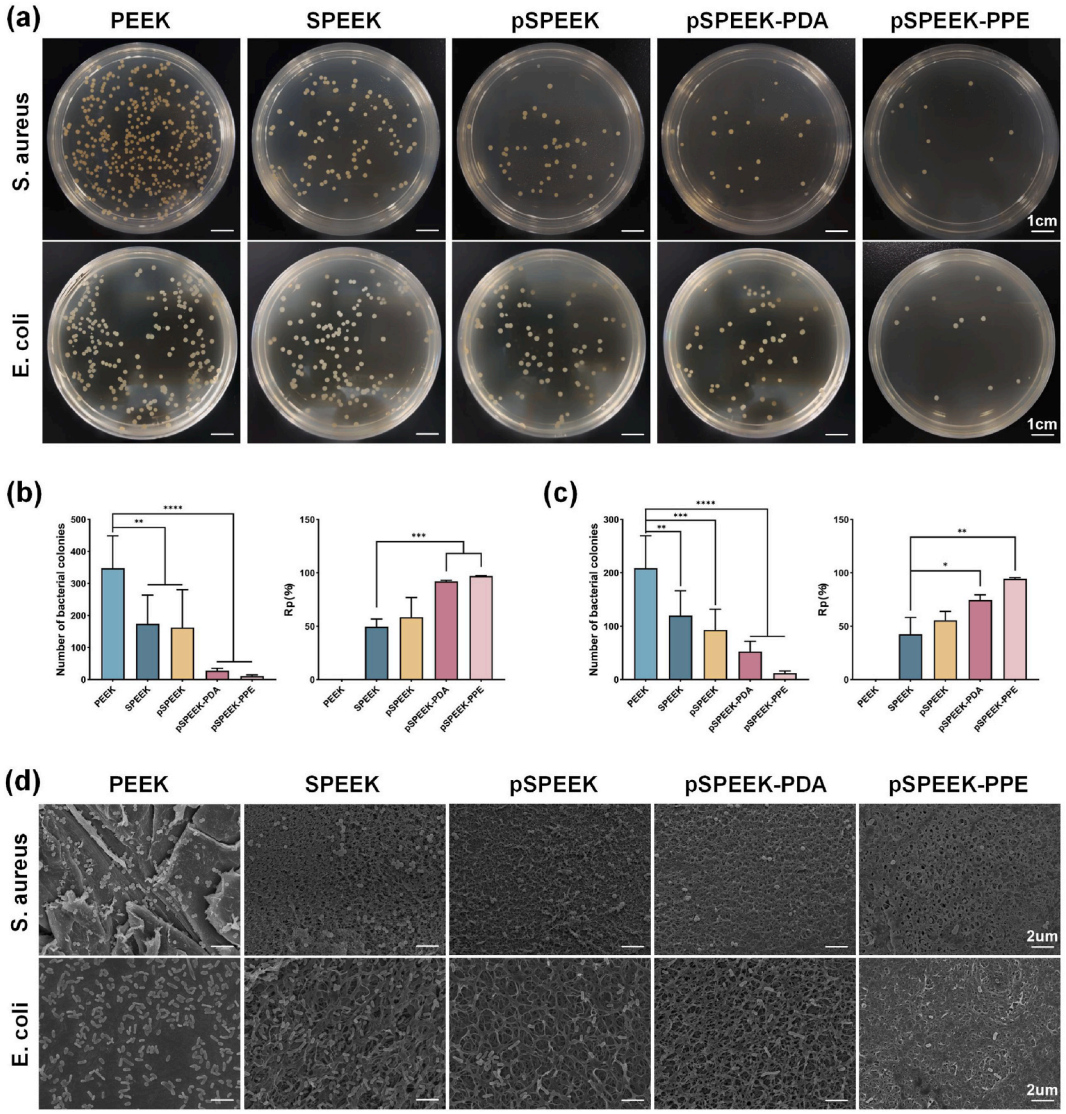

Fig. 6. S. aureus and E. coli adhesion on the specimens surface after 24 h: (a) optical images of cloned bacteria, (b) statistical count and antibacterial rate of S. aureus colonies, (c) statistical count and antibacterial rate of E. coli colonies, and (d) SEM images of S. aureus and E. coli statically cultured on various specimen surfaces, *P < 0.05, **P < 0.01, ***P < 0.001, ****P < 0.0001. Scale bars, 1 cm and 2 μm.

Initial cell-implant interactions might influence later cell differentiation and mineralization processes [40]. Consequently, genes such as ALP, OPN, Runx2, and Col1α1 were chosen to assess the osteogenic potential of modified PEEK in MC3T3-E1 preosteoblast cells using qRT-PCR. In comparison to the control PEEK group, MC3T3-E1 cells treated with pSPEEK-PPE demonstrated upregulated expression of these osteogenesis-related genes. The enhancement in ALP gene expression promotes phosphate formation, which are crucial for the development of prebone structures [25]. The upregulated Col1α1 genes are key for collagen secretion, which explains the formation of more calcium nodules on the surface of pSPEEK-PPE [26]. Additionally, the upregulated Runx2 genes are essential for the differentiation of osteogenic cells, especially in the process of transforming preosteoblasts into osteoblasts [41]. As implant biomaterials, it is crucial to possess the capacity to induce cell mineralization; thus, this study assessed whether the mineralization of cells cultured on modified specimen surfaces was enhanced, by measuring ALP activity and matrix mineralization at specific time points. ALP activity is an early osteogenic differentiation indicator [42]. On days 7 and 14 of culture, the pSPEEK-PPE surface notably induced the most intense alkaline phosphatase staining, with a high abundance of blue-violet positive cells, surpassing other groups. Likewise, matrix mineralization in the extracellular matrix on different PEEK surfaces was evaluated using AR staining at days 7 and 14, a marker of advanced osteogenic differentiation. Identified as red calcium deposits, these depositions are a late-stage osteogenic differentiation product [43]. Observations from AR staining revealed a pattern that aligns closely with the activity of ALP. Notably, the pSPEEK-PPE surface displayed a deep red hue over an extensive staining region, which suggests an elevated level of calcium. Overall, the ALP, AR staining, and RT-PCR results demonstrate consistent trends, indicating that phosphorylation of the surface promotes osteogenic

differentiation in MC3T3-E1 cells. Under physiological conditions, phosphate groups carry a negative charge, thus promoting the chelation of calcium ions, which plays a critical role in transmitting osteogenic signals [29,44]. Moreover, surfaces with negative charges are known to preferentially adsorb cell-adhesive proteins like fibronectin while reducing the adsorption of non-specific proteins such as albumin [29]. Observations indicate that the adhesion, spreading, proliferation, and differentiation of osteoblasts are significantly dependent on the presence of proteins like fibronectin and vitronectin, which are primarily adsorbed onto biomaterial surfaces [45]. These insights partially explain the improved responses of MC3T3-E1 cells on phosphorylated surfaces, though further studies are necessary to more accurately delineate the underlying mechanisms.

Prior research has established that infections related to implants are primarily due to microorganisms, particularly bacteria that adhere to the prosthetic surface [46]. Evidence suggests that the surface properties of the implant facilitate bacterial attachment, proliferation, and biofilm formation, thereby enhancing bacterial resistance to the body's antibacterial defenses [25]. In this study, Gram-negative E. coli and Gram-positive S. aureus were chosen as the model bacterial to explore the antibacterial properties of pSPEEK-PPE. Due to the introduction of polydopamine phosphate ester, the pSPEEK-PPE successfully suppressed the growth of both S. aureus and E. coli, according to the findings. The superior antibacterial characteristics of pSPEEK-PPE could partly be due to the retention of amino groups in polydopamine throughout the phosphorylation process. These groups are capable of forming electrostatic interactions with negatively charged elements on bacterial cell membranes, compromising their integrity [47]. This disruption leads to cellular imbalances that result in bacterial death. Furthermore, these amino groups have the ability to absorb and neutralize positively charged molecules on the surface of bacteria, thereby further suppressing their growth and proliferation [48]. On the other hand, the incorporation of 3D porous network and the application of polydopamine phosphate ester coating increase the roughness of the modified PEEK surface. Such textural changes could physically impede bacterial adhesion and biofilm development [34,40]. Additionally, the chemical structure of polydopamine phosphate ester may facilitate reactions with specific components within bacterial cell walls or membranes, such as proteins, lipids, or nucleic acids. These interactions could suppress bacterial vital functions or directly induce cell death. Elucidating the exact antibacterial mechanisms warrants further research, including assessments of cell membrane integrity or biofilm formation studies. Overall, the antibacterial mechanism of polydopamine phosphate ester-modified PEEK materials is multifaceted, involving a combination of physical, chemical, and biological properties. Even so, the polydopamine phosphate ester-modified 3D porous coating on PEEK introduces an innovative approach, potentially broadening its use in complex biomedical applications, particularly in oral and maxillofacial implants.

Previous research has explored the introduction of phosphate groups into PEEK either through a single-step process involving UV-initiated graft polymerization of vinyl phosphonic acid or by surface biphosphonation using alendronate [29,49]. These techniques have successfully enhanced the osteogenic properties of PEEK surfaces. Nevertheless, the preparation processes involved are somewhat complex and often result in unstable surface hydrophilicity. Moreover, the potential antibacterial properties of these modified surfaces have yet to be determined. In contrast to more intricate methods traditionally used to enhance biocompatibility and antibacterial properties, this study introduces a streamlined approach that leverages surface modification to meet these goals. The methodology entailed a straightforward process of immersing PEEK in various reaction solutions, thereby circumventing the need for complex and time-intensive chemical reactions that typically demand rigorous conditions and yield low productivity. This process began with the submersion of PEEK in concentrated sulfuric acid and subsequently in ultrapure water to create a 3D porous network on the surface. Oxygen plasma treatment was then applied to the sulfonated PEEK to activate its surface chemistry. A PDA coating was subsequently applied to the surface, furnishing active sites for phosphate group incorporation. The final step involved the spontaneous chemical bonding of phosphoryl chloride to the PDA layer under gentle conditions, thereby augmenting its bioactivity. It is important to note, however, that this study is confined to in vitro biological assessments, and its findings may not directly translate to in vivo contexts. Future research should also investigate its long-term efficacy. Additionally, an in-depth analysis of molecular pathways associated with this modification could offer substantial biological insights.

5. Conclusions

We achieved a synergistic enhancement of PEEK's biocompatibility and antibacterial properties through a series of surface modifications. The process, involving sulfonation, application of oxygen plasma, PDA coating, and the integration of phosphate groups, led to the creation of a polydopamine phosphate ester-modified 3D porous network on PEEK. This modification strategy significantly outperformed the control PEEK in promoting adhesion and proliferation of fibroblasts and osteoblasts, and in reducing the growth of S. aureus and E. coli, attributable to the newly introduced porous architecture and biomolecular coating. The resultant PEEK demonstrated marked improvements in biocompatibility, osteogenic induction, and antibacterial properties. These straightforward yet effective surface modifications suggest a promising avenue for advancing the use of PEEK in dental and maxillofacial implants. Nevertheless, in-depth investigations into the molecular mechanisms and in vivo studies are imperative to better understand the modified PEEK's role in long-term osseointegration and antibacterial efficacy within the organism.

Data availability

Data will be made available on request.

CRediT authorship contribution statement

Wenqing Meng: Conceptualization, Data curation, Formal analysis, Investigation, Methodology, Visualization, Writing – original

draft, Writing – review & editing. **Yifei Nie:** Data curation, Formal analysis, Investigation. **Jiajia Zhang:** Data curation, Visualization. **Ludan Qin:** Data curation, Visualization. **Xueye Liu:** Visualization. **Tongtong Ma:** Visualization. **Junling Wu:** Supervision, Writing – review & editing.

Declaration of competing interest

The authors declare that they have no known competing financial interests or personal relationships that could have appeared to influence the work reported in this paper.

Acknowledgments

This research did not receive any specific grant from funding agencies in the public, commercial, or not-for-profit sectors.

References

[1] Y. Liang, Y. Song, L. Wang, C. Wei, X. Zhou, Y. Feng, Research progress on antibacterial activity of medical titanium alloy implant materials, Odontology 111 (4) (2023) 813–829.
[2] L. Qin, S. Yao, J. Zhao, C. Zhou, T.W. Oates, M.D. Weir, J. Wu, H.H.K. Xu, Review on development and dental applications of polyetheretherketone-based biomaterials and Restorations, Materials 14 (2) (2021) 408.
[3] R. Huiskes, H. Weinans, B. van Rietbergen, The relationship between stress shielding and bone resorption around total hip stems and the effects of flexible materials, Clin. Orthop. Relat. Res. 274 (1992) 124–134.
[4] B.I. Oladapo, S.A. Zahedi, S.O. Ismail, F.T. Omigbodun, 3D printing of PEEK and its composite to increase biointerfaces as a biomedical material-A review, Colloids Surf. B Biointerfaces 203 (2021) 111726.
[5] S. Zhang, J. Long, L. Chen, J. Zhang, Y. Fan, J. Shi, Y. Huang, Treatment methods toward improving the anti-infection ability of poly (etheretherketone) implants for medical applications, Colloids Surf. B Biointerfaces 218 (2022) 112769.
[6] R. Ma, T. Tang, Current strategies to improve the bioactivity of PEEK, Int. J. Mol. Sci. 15 (4) (2014) 5426–5445.
[7] F.D. Al-Shalawi, A.H. Mohamed Ariff, D.W. Jung, M.K.A. Mohd Ariffin, C.L. Seng Kim, D. Brabazon, M.O. Al-Osaimi, Biomaterials as implants in the orthopedic field for regenerative medicine: metal versus synthetic polymers, Polymers 15 (12) (2023) 2601.
[8] T. Ma, J. Zhang, S. Sun, W. Meng, Y. Zhang, J. Wu, Current treatment methods to improve the bioactivity and bonding strength of PEEK for dental application: a systematic review, Eur. Polym. J. 183 (2023) 111757.
[9] X. Meng, J. Zhang, J. Chen, B. Nie, B. Yue, W. Zhang, Z. Lyu, T. Long, Y. Wang, KR-12 coating of polyetheretherketone (PEEK) surface via polydopamine improves osteointegration and antibacterial activity in vivo, J. Mater. Chem. B 8 (44) (2020) 10190–10204.
[10] I. Uysal, A. Tezcaner, Z. Evis, Methods to improve antibacterial properties of PEEK: a review, Biomedical materials (Bristol, England) 19 (2) (2024), https://doi.org/10.1088/1748-605X/ad2a3d.
[11] T. Chen, Y. Jinno, I. Atsuta, A. Tsuchiya, M. Stocchero, E. Bressan, Y. Ayukawa, Current surface modification strategies to improve the binding efficiency of emerging biomaterial polyetheretherketone (PEEK) with bone and soft tissue: a literature review, Journal of prosthodontic research 67 (3) (2023) 337–347.
[12] L. Zhao, J. Hu, L. Gao, J. Wang, X. Ma, Y. Liu, Y. Ao, F. Yan, L. Liu, Improvement of interfacial properties and bioactivity of CF/PEEK composites by rapid biomineralization of hydroxyapatite, ACS Biomater. Sci. Eng. 9 (7) (2023) 4117–4125.
[13] J. Li, J. Li, Y. Yang, X. He, X. Wei, Q. Tan, Y. Wang, S. Xu, S. Chang, W. Liu, Biocompatibility and osteointegration capability of β-TCP manufactured by stereolithography 3D printing: in vitro study, Open Life Sci. 18 (1) (2023) 20220530.
[14] M.S. Abu Bakar, M.H. Cheng, S.M. Tang, S.C. Yu, K. Liao, C.T. Tan, K.A. Khor, P. Cheang, Tensile properties, tension-tension fatigue and biological response of polyetheretherketone-hydroxyapatite composites for load-bearing orthopedic implants, Biomaterials 24 (13) (2003) 2245–2250.
[15] R.J. Mobbs, T. Amin, D. Ho, A. McEvoy, V. Lovric, W.R. Walsh, Integral fixation titanium/polyetheretherketone cages for cervical arthrodesis: two-year clinical outcomes and fusion rates using β-tricalcium phosphate or supercritical carbon dioxide treated allograft, J. Craniovertebral Junction Spine 12 (4) (2021) 368–375.
[16] Z. Zheng, P. Liu, X. Zhang, Jingguo Xin, Yongjie Wang, X. Zou, X. Mei, S. Zhang, S. Zhang, Strategies to improve bioactive and antibacterial properties of polyetheretherketone (PEEK) for use as orthopedic implants, Materials today. Bio 16 (2022) 100402.
[17] R. Ma, J. Wang, C. Li, K. Ma, J. Wei, P. Yang, D. Guo, K. Wang, W. Wang, Effects of different sulfonation times and post-treatment methods on the characterization and cytocompatibility of sulfonated PEEK, J. Biomater. Appl. 35 (3) (2020) 342–352.
[18] Y. Zhao, H.M. Wong, W. Wang, P. Li, Z. Xu, E.Y. Chong, C.H. Yan, K.W. Yeung, P.K. Chu, Cytocompatibility, osseointegration, and bioactivity of three-dimensional porous and nanostructured network on polyetheretherketone, Biomaterials 34 (37) (2013) 9264–9277.
[19] X. Han, N. Sharma, S. Spintzyk, Y. Zhou, Z. Xu, F.M. Thieringer, F. Rupp, Tailoring the biologic responses of 3D printed PEEK medical implants by plasma functionalization, Dent. Mater. : official publication of the Academy of Dental Materials 38 (7) (2022) 1083–1098.
[20] D. Briem, S. Strametz, K. Schröder, N.M. Meenen, W. Lehmann, W. Linhart, A. Ohl, J.M. Rueger, Response of primary fibroblasts and osteoblasts to plasma treated polyetheretherketone (PEEK) surfaces. Journal of materials science, Materials in medicine 16 (7) (2005) 671–677.
[21] J. Waser-Althaus, A. Salamon, M. Waser, C. Padeste, M. Kreutzer, U. Pieles, B. Müller, K. Peters, Differentiation of human mesenchymal stem cells on plasma-treated polyetheretherketone. Journal of materials science, Materials in medicine 25 (2) (2014) 515–525.
[22] Q. Fu, M. Gabriel, F. Schmidt, W.D. Müller, A.D. Schwitalla, The impact of different low-pressure plasma types on the physical, chemical and biological surface properties of PEEK, Dent. Mater. : official publication of the Academy of Dental Materials 37 (1) (2021) e15–e22.
[23] P. Sundriyal, M. Sahu, O. Prakash, S. Bhattacharya, Long-term surface modification of PEEK polymer using plasma and PEG silane treatment, Surface. Interfac. 25 (2021) 101253.
[24] L. Ma, G. Li, J. Lei, Y. Song, X. Feng, L. Tan, R. Luo, Z. Liao, Y. Shi, W. Zhang, X. Liu, W. Sheng, S. Wu, C. Yang, Nanotopography sequentially mediates human mesenchymal stem cell-derived small extracellular vesicles for enhancing osteogenesis, ACS Nano 16 (1) (2022) 415–430.
[25] X. Yang, Q. Wang, Y. Zhang, H. He, S. Xiong, P. Chen, C. Li, L. Wang, G. Lu, Y. Xu, A dual-functional PEEK implant coating for anti-bacterial and accelerated osseointegration, Colloids and surfaces B, Biointerfaces 224 (2023) 113196.
[26] Y. Zhu, Z. Cao, Y. Peng, L. Hu, T. Guney, B. Tang, Facile surface modification method for synergistically enhancing the biocompatibility and bioactivity of poly (ether ether ketone) that induced osteodifferentiation, ACS Appl. Mater. Interfaces 11 (31) (2019) 27503–27511.
[27] N. Fukuda, M. Kanazawa, K. Tsuru, A.Sunarso Tsuchiya, R. Toita, Y. Mori, Y. Nakashima, K. Ishikawa, Synergistic effect of surface phosphorylation and micro-roughness on enhanced osseointegration ability of poly(ether ether ketone) in the rabbit tibia, Sci. Rep. 8 (1) (2018) 16887.
[28] N. Fukuda, A.Sunarso Tsuchiya, R. Toita, K. Tsuru, Y. Mori, K. Ishikawa, Surface plasma treatment and phosphorylation enhance the biological performance of poly(ether ether ketone), Colloids and surfaces B, Biointerfaces 173 (2019) 36–42.
[29] Y. Zheng, L. Liu, L. Xiao, Q. Zhang, Y. Liu, Enhanced osteogenic activity of phosphorylated polyetheretherketone via surface-initiated grafting polymerization of vinylphosphonic acid, Colloids and surfaces B, Biointerfaces 173 (2019) 591–598.
[30] H. Lyu, N. Jiang, J. Hu, Y. Li, N. Zhou, D. Zhang, Preparing water-based phosphorylated PEEK sizing agent for CF/PEEK interface enhancement, Compos. Sci. Technol. 217 (2022) 109096.

[31] Z. Wang, X. Zhang, S. Yao, J. Zhao, C. Zhou, J. Wu, Development of low-shrinkage dental adhesives via blending with spiroorthocarbonate expanding monomer and unsaturated epoxy resin monomer, J. Mech. Behav. Biomed. Mater. 133 (2022) 105308.
[32] L. Qin, S. Yao, W. Meng, J. Zhang, R. Shi, C. Zhou, J. Wu, Novel antibacterial dental resin containing silanized hydroxyapatite nanofibers with remineralization capability, Dent. Mater. : official publication of the Academy of Dental Materials 38 (12) (2022) 1989–2002.
[33] S. Yao, L. Qin, Z. Wang, L. Zhu, C. Zhou, J. Wu, Novel nanoparticle-modified multifunctional microcapsules with self-healing and antibacterial activities for dental applications, Dent. Mater. : official publication of the Academy of Dental Materials 38 (8) (2022) 1301–1315.
[34] P. Xian, Y. Chen, S. Gao, J. Qian, G. Wan, Polydopamine (PDA) mediated nanogranular-structured titanium dioxide (TiO2) coating on polyetheretherketone (PEEK) for oral and maxillofacial implants application, Surf. Coating. Technol. 401 (2020) 126282.
[35] S. Sadhwani, A. Kamson, A.J. Frear, N. Sadaka, K.L. Urish, Current concepts on the clinical and economic impact of periprosthetic joint infections, Orthop. Clin. N. Am. 55 (2) (2024) 151–159.
[36] V. Karageorgiou, D. Kaplan, Porosity of 3D biomaterial scaffolds and osteogenesis, Biomaterials 26 (27) (2005) 5474–5491.
[37] F. Xiao, Y. Zhai, Y. Zhou, X. Xu, W. Wang, Low-temperature fabrication of titania layer on 3D-printed PEKK for enhancing biocompatibility, Surf. Coating. Technol. (37) (2021) 127158.
[38] S.W. Ha, R. Hauert, K.H. Ernst, E. Wintermantel, Surface analysis of chemically-etched and plasma-treated polyetheretherketone (PEEK) for biomedical applications, Surf. Coating. Technol. 96 (2–3) (1997) 293–299.
[39] L. Bacakova, E. Filova, M. Parizek, T. Ruml, V. Svorcik, Modulation of cell adhesion, proliferation and differentiation on materials designed for body implants, Biotechnol. Adv. 29 (6) (2011) 739–767.
[40] T. Stich, F. Alagboso, T. Křenek, T. Kovářík, V. Alt, D. Docheva, Implant-bone-interface: reviewing the impact of titanium surface modifications on osteogenic processes in vitro and in vivo, Bioengineering & translational medicine 7 (1) (2021) e10239.
[41] C. Gao, Z. Wang, Z. Jiao, Z. Wu, M. Guo, Y. Wang, P. Zhang, Enhancing antibacterial capability and osseointegration of polyetheretherketone (PEEK) implants by dual-functional surface modification, Mater. Des. 205 (2021) 109733.
[42] Z. Yuan, B. Tao, Y. He, C. Mu, G. Liu, J. Zhang, Q. Liao, P. Liu, K. Cai, Remote eradication of biofilm on titanium implant via near-infrared light triggered photothermal/photodynamic therapy strategy, Biomaterials 223 (2019) 119479.
[43] H. Gu, F. Guo, X. Zhou, L. Gong, Y. Zhang, W. Zhai, L. Chen, L. Cen, S. Yin, J. Chang, L. Cui, The stimulation of osteogenic differentiation of human adipose-derived stem cells by ionic products from akermanite dissolution via activation of the ERK pathway, Biomaterials 32 (29) (2011) 7023–7033.
[44] A.S. Wagner, K. Glenske, V. Wolf, D. Fietz, S. Mazurek, T. Hanke, A. Moritz, S. Arnhold, S. Wenisch, Osteogenic differentiation capacity of human mesenchymal stromal cells in response to extracellular calcium with special regard to connexin 43, Annals of anatomy = Anatomischer Anzeiger : official organ of the Anatomische Gesellschaft 209 (2017) 18–24.
[45] L.F. Mellor, M. Mohiti-Asli, J. Williams, A. Kannan, M.R. Dent, F. Guilak, E.G. Loboa, Extracellular calcium modulates chondrogenic and osteogenic differentiation of human adipose-derived stem cells: a novel approach for osteochondral tissue engineering using a single stem cell source. Tissue engineering, Part A 21 (17–18) (2015) 2323–2333.
[46] Z. Su, L. Kong, Y. Dai, J. Tang, J. Mei, Z. Qian, Y. Ma, Q. Li, S. Ju, J. Wang, W. Fan, C. Zhu, Bioresponsive nano-antibacterials for H2S-sensitized hyperthermia and immunomodulation against refractory implant-related infections, Sci. Adv. 8 (14) (2022) eabn1701.
[47] Z. Xu, T. Wang, J. Liu, Recent development of polydopamine anti-bacterial nanomaterials, Int. J. Mol. Sci. 23 (13) (2022) 7278.
[48] J. Zhou, Y. Cai, Y. Liu, H. An, K. Deng, M.A. Ashraf, L. Zou, J. Wang, Breaking down the cell wall: still an attractive antibacterial strategy, Front. Microbiol. 13 (2022) 952633.
[49] W. Zhang, L. Liu, H. Zhou, C. He, X. Yang, J. Fu, Y. Zheng, Surface bisphosphonation of polyetheretherketone to manipulate immune response for advanced osseointegration, Mater. Des. 232 (2023) 112151.